

PAPER



Cite this: *Sustainable Energy Fuels*, 2020, 4, 1773

Received 23rd November 2019
Accepted 6th January 2020

DOI: 10.1039/c9se01141b

rsc.li/sustainable-energy

Methanol production from CO₂ via an integrated, formamide-assisted approach†

Jorge G. Uranga,^{‡*ab} Aswin Gopakumar,^{‡a} Tim Pfister,^{‡a} Gunay Imanzade,^a Loris Lombardo,^{‡acd} Gabriela Gastelu,^b Andreas Züttel^{cd} and Paul J. Dyson^{‡*a}

The synthesis of fuels from CO₂ has made tremendous progress in recent years, although practical applications remain limited. Herein, we describe a cyclic process that produces MeOH from CO₂ via formamide intermediates, which are initially reduced using NaBH₄ to form methanol and concomitantly release the corresponding amine, from which the formamide is subsequently regenerated in the presence of CO₂/NaBH₄. By tuning the substituents on the formamide/amine, the selectivity of both steps can be controlled, allowing the process to proceed in high yields, either in two separate steps or in a single step process. The observed trends in reactivity were rationalized with a resonance model of the formamide, which supports the observed trends in reactivity, and further consolidated by spectroscopy and calculations.

Introduction

The accumulation of anthropogenic CO₂ in the atmosphere is a major contributor to global warming and poses one of the greatest challenges facing society today. Anthropogenic activities concerned primarily with transportation, electricity production, the cement industry, and uncontrolled deforestation have led to the spiraling increase and accumulation of CO₂ in the Earth's biosphere. The reduction of CO₂ generally requires a catalyst to lower the high activation barrier associated with the process, with sustainable reaction pathways that afford MeOH (which may be used directly as a fuel, or as a fuel-additive and also as a versatile synthon) being particularly attractive.¹ Numerous reports have described the direct hydrogenation of CO₂ to MeOH using molecular hydrogen as the reducing agent employing catalysts based on Ru,^{2–4} Pd,^{5–9} Rh^{10,11} and Mn¹² that operate under relatively harsh conditions. An alternative reaction pathway involves the reduction of organic carrier molecules including carbonates,^{2,13–15} carbamates,² urea derivatives,¹⁶ formates,² amides^{17–20} and formamides²¹ to afford

methanol. Such carbonyl compounds are known to be challenging to reduce.²² Among them, however, the formamide reduction approach is gaining increasing attention as highly efficient and straightforward protocols have been reported for the *N*-formylation of amines.^{23–27}

The pioneering work from Milstein and co-workers described the direct hydrogenation of *N*-formylmorpholine to methanol and morpholine employing a bipyridyl-based PNN Ru(II) pincer complex catalyst.¹⁷ Subsequently, other catalysts were reported for this reaction.^{20,28} However, the reaction requires additives and as harsh reaction conditions are used the selectivity is low, *e.g.*, in the presence of groups such as –NO₂, –OMe, *etc.* To the best of our knowledge, the use of a conventional transfer hydrogenation agent such as borohydrides has not been investigated in CO₂-based *N*-formylations and their subsequent reduction to methanol. Interestingly, a report in 1993 described the reduction of *N,N*-dimethylformamide (DMF) to trimethylamine and bis(dimethylamino)methane using sodium borohydride.²⁹ Zinc borohydride also efficiently reduces amides.³⁰ Very recently, an attractive approach to capture and transform atmospheric CO₂ to formate and formoxyborane (and then to methanol through hydrolysis) under ambient conditions using an intricate system based on *N*-heterocyclic carbenes (NHCs) and boranes has been reported.³¹

It is noteworthy that borohydrides are known to capture and functionalize CO₂ under ambient conditions to yield triformatoborohydrides,³² which are involved in the formylation of amines using CO₂ and NaBH₄.³³ It has also been shown that NaBH₄ can reduce carbonyl compounds, *e.g.*, aldehydes and ketones.³⁴ Considering the low costs of borohydrides,^{35,36} their relatively high stability, hydrogen content, and less stringent safety and storage requirements, we decided to explore the use

^aInstitute of Chemical Sciences and Engineering (ISIC), École Polytechnique Fédérale de Lausanne (EPFL), Lausanne-1015, Switzerland. E-mail: jorge.uranga@unc.edu.ar; paul.dyson@epfl.ch

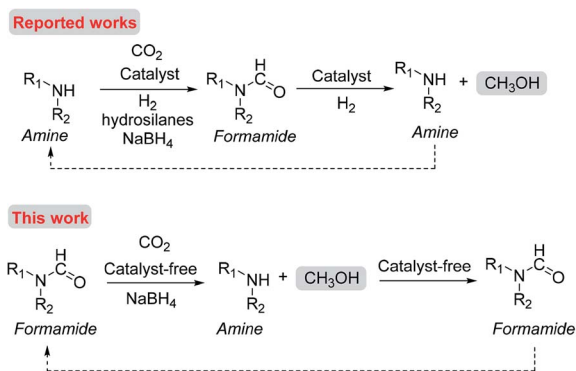
^bDepartamento de Química Orgánica, Facultad de Ciencias Químicas, UNC, Instituto de Investigaciones en Físicoquímica de Córdoba (INFIQC-CONICET), Córdoba, 5000, Argentina

^cInstitute of Chemical Sciences and Engineering (ISIC), École Polytechnique Fédérale de Lausanne (EPFL), CH-1951 Sion, Switzerland

^dEMPA Materials Science and Technology, Dübendorf-8600, Switzerland

† Electronic supplementary information (ESI) available: Additional synthesis, NMR and computational data. See DOI: 10.1039/c9se01141b

‡ Equal contribution to this work.



Scheme 1 Reaction pathways showing the conversion of CO₂ to MeOH using amines/formamides as relay molecules.

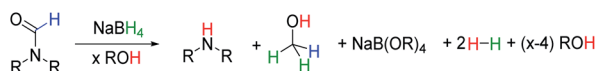
of NaBH₄ to reductively cleave the carbonyl C–N bond in formamides to generate the parent amine and methanol as shown in Scheme 1, and ultimately to design a simple route to transform CO₂ into MeOH. Subsequently, we describe a straightforward approach to rationalize and predict the reactivity amines/formamides employed in the process and show that electronic effects significantly impact on the reactivity.

Results and discussion

Reduction of formamides

Initially, the reduction of *N,N*-diphenylformamide (**1a**) with NaBH₄ was investigated as a model reaction in different protic solvents. The requirement for a proton source is evident from the reaction shown in Scheme 2. Note that the observed reactivity differs significantly depending on the proton source (Table S1, ESI†).

Employing diethylene glycol (DEG) as the solvent results in the rapid conversion of **1a** under mild conditions. However, diethylene glycol also reacts rapidly with NaBH₄, leading to hydrogen gas evolution *via* the known alcoholysis reaction.³⁷ Consequently, three equivalents of NaBH₄ relative to the formamide were required for full conversion since part of the NaBH₄ is directly consumed by the solvent. This side reaction between the solvent with NaBH₄ (alcoholysis) was found to be the main reaction for the other alcohols tested, *i.e.*, methanol, ethanol, and *tert*-butanol, (Table S1, ESI†). In contrast, the reduction was achieved efficiently with 0.8 equivalents of NaBH₄ using water as the proton source in combination with DMSO (DMSO was chosen because of its high boiling point and its ability to dissolve the substrates and intermediates), although the reaction proceeds more slowly than in alcohols, DEG and water/THF mixture (Fig. S1, ESI†). Since the reactivity of *N,N*-diphenylformamide is very high, a substrate with intermediate reactivity, *i.e.*, *N*-methylformanilide, was used for further

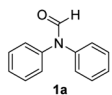
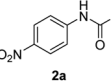
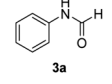
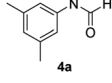
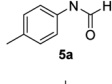
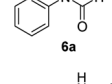
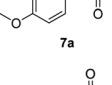
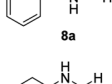
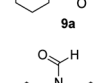
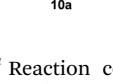


Scheme 2 Reduction of formamides with NaBH₄ in protic solvents.

optimizations. The DMSO : water ratio was investigated, with 15 vol% water giving the fastest rates, with higher levels of water leading to faster hydrolysis of NaBH₄ (Table S2 and Fig. S2, ESI†). The reaction was studied at different temperatures with the optimum yield obtained at 90 °C (Table S3 and Fig. S3, ESI†). Selective formamide reduction was observed using DMSO (2 mL with 15 vol% water), NaBH₄ (0.8–1.8 equivalents) at 90 °C, and the scope of the reaction was investigated using these conditions (Table 1).

Exceptional reactivity was observed with substrates **1a** and **2a**, achieving near quantitative conversion after 1 and 2 h, respectively. Moreover, with these substrates, only 0.7 equivalents of NaBH₄ was required. In comparison, substrates **3a–7a** bearing an unsubstituted aryl or an aryl group with weakly

Table 1 Substrate scope for the reduction of formamides^a

Substrate	Time (h)	Conversion ^b (%)	Amine ^b (%)	Methanol ^b (%)
	2	99+	99+	62
	1	99+	99+	72
	8	87	85	69
	8	77	77	64
	8	72	66	55
	8	69	66	52
	8	61	57	47
	8	13	10	8
	8	0	0	0
	8	0	0	0

^a Reaction conditions: formamide (1.0 mmol), DMSO/water (2 mL, 15 vol% H₂O), 90 °C, NaBH₄ (1.7 equivalents); except for substrate **1b** where 0.8 equivalent borohydride was required. 8 h was selected as the reaction time which is sub-optimal, but allows clear differences in reactivity to be ascertained. ^b Yield determined by ¹H NMR spectroscopy using mesitylene as an internal standard. See Fig. S4–S11, ESI for the ¹H NMR spectroscopic quantification of the amines.

electron-donating substituents (EDG) showed intermediate reactivity and lower conversions. Benzylic (**8a**) and aliphatic formamides (**9a** and **10a**) with EDGs were transformed under the same reaction conditions. The general reactivity trend is similar to that reported for formamide hydrogenation.²⁰ The relative methanol yields were found to be proportional to the total substrate conversion, and the difference in the amine yield and (lower) amount of methanol obtained is presumably due to the formation of formatoborohydride (at ~8.4 ppm), which is detected by NMR spectroscopy (Fig. S2, ESI†).

Formylation of amines

Having explored the reduction of formamides, we explored a compatible formylation procedure to regenerate the starting formamides employing carbon dioxide as a C1 source. The *N*-formylation of secondary amines has recently been described using CO₂ and NaBH₄ via a triformatoborohydride intermediate that acts as the formylating agent.³³ Consequently, the synthesis of sodium triformatoborohydride was carried out before the addition of the amine (Scheme 3), and the resulting homogeneous solution was used as a 'formylation reagent'.

With this approach, it was possible to formylate several amines under milder conditions than those employed in the previous report.³³ The substrate scope for the *N*-formylation reaction is presented in Table 2 and the observed trend in reactivity for the *N*-formylation is essentially the opposite of that observed for the reduction step, *i.e.*, amines with strong electron-withdrawing substituents (EWGs) (**1b**, **2b**) did not react whereas amines with EDGs (**4b**, **6b**, **7b**) readily reacted within a few hours affording the desired products in high yield. Notably, benzylamine and cyclohexylamine (**8b**, **9b**) were the most reactive amines evaluated. These results are consistent with previous reports concerned with *N*-formylation reactions.^{23,38,39} The products were purified using a simple extraction procedure involving ethyl acetate/water (see Experimental). To decipher the fate of the boron atom in NaBH₄, ¹¹B NMR spectroscopy was used to analyze the system before and after reaction employing a representative substrate, **6a**. The appearance of a broad peak at ~5 ppm after the reduction step indicates the formation of hydroborate, *i.e.* [NaBH_{4-x}(OH)_x] (Fig. S12, ESI†).

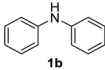
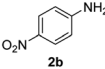
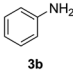
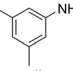
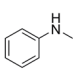
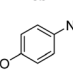
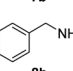
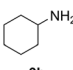
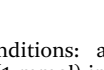
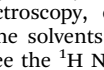
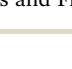
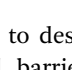
Spectroscopic and DFT studies

Due to the strong influence of the substrate on the reactivity, comprehensive analysis of the structure and electronic factors is crucial to understand and develop suitable processes for sustainable methanol production from CO₂ using amine/formamide relay molecules. Therefore, we investigated the structure–reactivity relationships of the formamides, since they are the key intermediates. The amide resonance model is



Scheme 3 Stepwise *N*-formylation of amines via a triformatoborohydride intermediate.

Table 2 Substrate scope for the *N*-formylation of amines^a

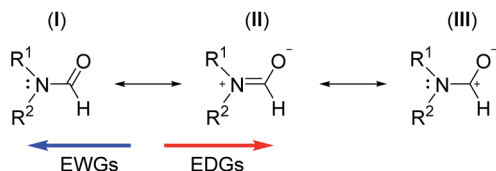
Entry	Substrate ^a	Time (h)	Formamide ^b (%)
1		4	0
2		4	0
3		4	43
4		2	48
5		4	88
6		5	97 (92) ^c
7		2	26
8		4	46
9		2	54
10		4	96 (90) ^c
11		2	97 (93) ^c
12		2	ND (95) ^c

^a Reaction conditions: amine (1.0 mmol), triformatoborohydride/activated CO₂ (1 mmol) in DMSO (1 mL), 70 °C. ^b Yield determined by ¹H NMR spectroscopy, except for substrate **9b** whose H signals overlap with the solvents (ND = not determined). ^c Isolated yield in parenthesis. See the ¹H NMR spectra in the ESI, Fig. S13–S17, for the reaction mixtures and Fig. S18–S21 for the isolated products.

generally used to describe their properties, such as geometry and rotational barrier [resonance structures (I) and (II) in Scheme 4].⁴⁰ Alternatively, a polarization model [structure (III) in Scheme 4] has also been used to rationalize their properties.^{40,41} The electronic properties of the amide bond are expected to be influenced by substituents (R¹ and R², Scheme 4) since they affect the contribution of each canonical structure concerning the overall resonance hybrid. EWGs favor the type I structure, whereas EDGs favor the type II structure. In some cases, when conjugation is not observed, the type III structure is the most representative.

The substituents are expected to significantly influence the carbonyl stretching frequency (ν_{CO}), as previously observed for lactams.⁴² Changes in ν_{CO} may be attributed to an intrinsic change in the carbonyl stretching force constant, and if the nitrogen lone pair does not participate, a type III structure will prevail. However, a change in the interaction between the carbonyl group and the neighboring nitrogen results in type I and II resonance structures depending on the electronic properties of the substituent.

Since the magnitude of a stretching force constant can be qualitatively related to the strength of a bond, any variation in bond order due to the electronic properties of the substituents



Scheme 4 Resonance structures of formamides.

should be reflected in the value of ν_{CO} . Consequently, the IR spectra of the formamides shown in Fig. 1a were recorded in DMSO. The ν_{CO} peaks (Fig. 1b) confirm the strong influence of the electronic properties of the substituents as significant differences in the stretching frequencies are observed. The presence of EWGs localizes the nitrogen lone pair avoiding the

polarization present in the type II structure. Instead, resonance structure type I is dominant and can be considered as a ‘carbonyl-amine’ (see 1a and 3a stretches in Fig. 1b). This electronic configuration is evidenced by a stronger C=O bond with the ν_{CO} observed at higher energies with the wavenumber values being close to that of an aldehyde, *i.e.*, 1705 cm^{-1} for phenylacetaldehyde.⁴³ In contrast, EDGs decrease the ν_{CO} value (see 8a, 9a and 10a stretch in Fig. 1b), which is expected for a type II resonance structure, and as the C=O bond order decreases the C–N bond order increases.

The observed IR stretches of the formamides are in agreement (disregarding steric factors) with the observed reactivity, *i.e.*, the more electron-rich the C=O bond, the more reactive the formamide. Complementary information was acquired from ^1H NMR spectroscopy since the electron density at the carbonyl group affects the chemical shift of the formyl proton (C^1HO), the values of which are schematically represented in Fig. 1c (spectra were recorded in DMSO- d_6). Considering the possibility of two conformers (*cis* and *trans*) in secondary formamides, the average of both values was used to estimate the overall effect of the induced field [(chemical shift (δ) of *cis*-conformer + chemical shift (δ) of *trans*-conformer)/2].

The carbonylic proton in formamides with EWGs is observed above 8.4 ppm, which is expected due to the high degree of electron density on the carbonyl group. In contrast, the carbonylic proton in formamides with strong EDGs appears around 8.0 ppm, consistent with the type II resonance structure favored by these formamides, and the lower electron density associated with the carbonyl moiety. The averaged chemical shifts of the carbonyl proton correlate well with the observed reactivity for the reduction and formylation, independent of the degree of substitution. Hence, the more electron-rich the carbonyl bond, the higher the ^1H NMR chemical shift and *vice versa*. This change in chemical shift is expected considering the induced magnetic field originated by C=O bond which directly affects the neighboring proton (C^1HO), deshielding the ^1H to a greater extent when the C=O bond is more electron rich, and in a lesser extent when the carbonyl group is electron-poor. Overall, the chemical shifts of the formyl proton correlate more closely with the reactivity of formamides in both the formylation and the reduction reaction steps compared to the IR ν_{CO} values.

Additionally, calculations were performed to further rationalize the spectroscopic data. The electronic properties of the formamide bonds were calculated using the Natural Bond Orbital (NBO) model. The calculated atomic charge on the carbonyl oxygen and the bond order analysis are included in Fig. 1d. For formamides with EDGs, the negative charge on the oxygen atom and C–N bond order are predicted to be high, which is in agreement with the dipolar resonance structure type II. In the case of formamides with EWGs, a low anionic charge on the oxygen and a low C–N bond order were calculated that matches with the lower conjugation between the nitrogen lone pair and the carbonyl bond. The calculations confirm that the formamide resonance model describes the reactivity more accurately than the polarization model. More detailed spectroscopic and theoretical analyses are presented in Table S4, ESI.†

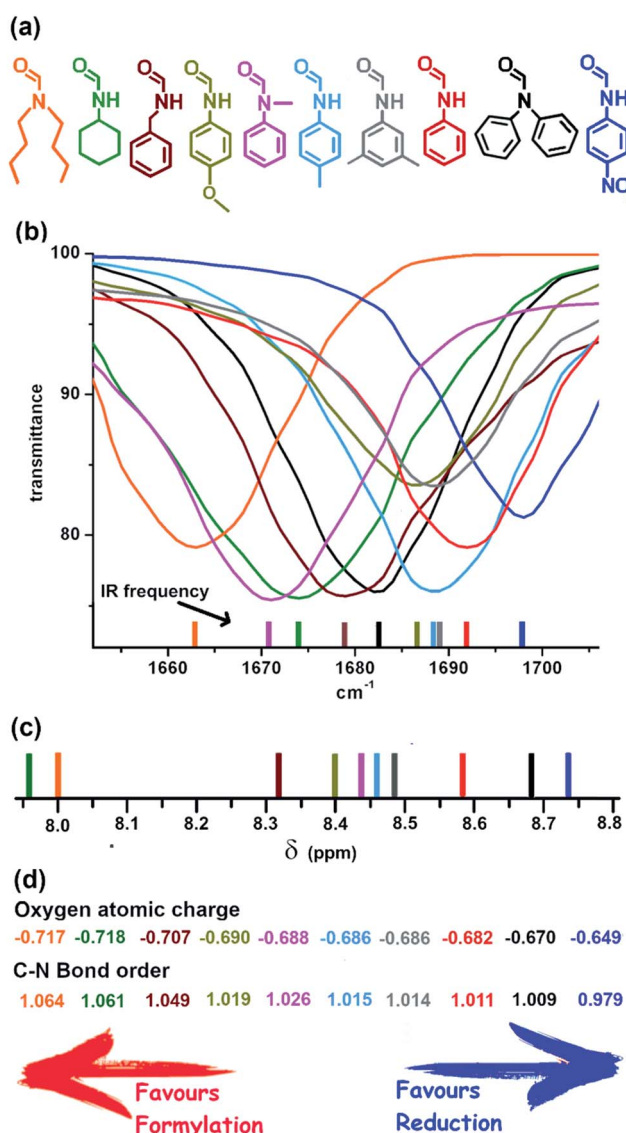
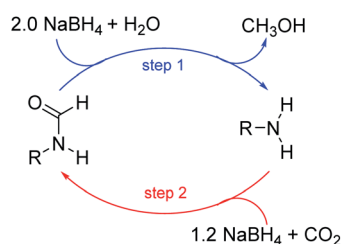


Fig. 1 Spectroscopic and computational data of formamides (labeled using colors): (a) investigated formamides, (b) ν_{CO} bands, (c) chemical shift of the carbonylic proton and (d) the calculated oxygen atomic charges and C–N bond orders. Separated IR spectra of the formamides are provided in Fig. S22, ESI.†

Formamides with EDGs favor resonance structure type II, leading to a decrease in the carbonyl electron density and an increase in the atomic charge on the oxygen and in the C–N bond order. As a result, the formamide is more stable favoring the formylation reaction and disfavoring the reduction reaction. In the case of EWGs, resonance structure type I is predominant, destabilizing the formamide and thus favoring the reduction reaction while disfavoring the formylation reaction. Notably, the averaged chemical shift of carbonylic proton can be used to predict the observed yield in the formylation (under a wide range of experimental conditions). Electrostatic potential (ESP) maps of the formamides showing the conjugation effect induced by different substituent groups are provided in Fig. S23, ESI.†

Tandem protocol

Based on the structure–reactivity analysis, formamides with moderate reactivity in both the *N*-formylation and reduction reactions such as formanilide (3a), 4-methylformanilide (5a) and 4-methoxyformanilide (7a) were later employed in the tandem strategy displayed in Scheme 5. These substrates are susceptible to reduction and reformylation. Here, the initial reduction of the



Scheme 5 Tandem reduction–formylation of formamides.

Table 3 Tandem reduction–formylation reactions^a

Substrate ^a	Step 1		Step 2
	Amine yield ^b [%]	Methanol yield ^b [%]	Formamide (recovered) yield ^b [%]
	96	74	74
	99	73	89
	79	64	96

^a Reaction conditions. Step 1: formamide (1.0 mmol), DMSO/water (2 mL, 15 vol% water), 90 °C, 16 h, NaBH₄ (2 equivalents). Step 2: triformatoborohydride (1.2 M in 0.8 mL DMSO), 100 °C, 12 h. ^b Yield determined by ¹H NMR spectroscopy using mesitylene as internal standard. ¹H NMR spectra are provided in Fig. S24–S26, ESI.

formamides (step 1) was followed by *in situ* formylation (step 2) of the resulting amine (see Table 3). Slightly modified conditions were used in the one-pot procedure to raise the yield in the reduction step (*i.e.*, longer reaction times and two equivalents of NaBH₄). Note that the excess H₂O in the solution lowers the reactivity for the formylation (step 2), probably due to hydrogen bonding with the amine that hinders nucleophilic attack due to solvation. By removing the water, the formylation step proceeds in high yield (Table 3). Integrated protocols employing the catalytic hydrogenation of formamides have been reported, but these processes require high temperatures and pressures (above 110 °C and 40 bar pressure) and employ metal catalysts.^{3,12,21} Here, by employing the optimum amine, methanol is obtained from CO₂ under milder conditions.

Experimental

Materials and methods

Reagents and solvents were obtained from commercial sources and used without further purification. Technical grade CO₂ was obtained from Carbagas AG. ¹H and ¹³C NMR spectra were recorded on a Bruker DMX 400 NMR spectrometer at 400 MHz (¹H) and 100 MHz (¹³C) in DMSO-*d*₆. Fourier-transform infrared (FT-IR) spectra were recorded on a PerkinElmer FT-IR 2000 instrument diluted in DMSO (1 M). All the characteristic NMR peaks for substrates and products were compared to literature data^{44,45} and/or authentic samples.

General procedure for the reduction of formamides

The reduction of formamides was carried out by dissolving the appropriate formamide (1 mmol) in DMSO/water (1.7 mL of DMSO-*d*₆ and 0.3 mL of double-distilled water). The reaction was maintained at 90 °C for the indicated time. Subsequently, the reaction was cooled in a water bath for 30 min, and the pressure was slowly released using a needle. Mesitylene (approximately 0.85 equivalents) was added to the reaction mixture as an internal standard. A sample was taken and diluted in DMSO-*d*₆ to quantify by NMR spectroscopy. The yields were determined by ¹H NMR spectroscopy from the integration ratios between aromatic peaks of the amine formed and the aromatic mesitylene singlet at ~6.7 ppm and/or the aliphatic mesitylene peak ~2.2 ppm.

General procedure for the formylation of amines

The *N*-formylation reaction was performed after activating the CO₂ (triformatoborohydride synthesis). A stock solution of triformatoborohydride was prepared in a closed microwave vial by dissolving NaBH₄ (5 mmol) in dry DMSO (5 mL) and then pressurizing with CO₂ (20 bars). The reaction was maintained at 60 °C for a period of 3 h yielding a homogeneous solution of HB(O(O)CH)₃. The ¹H NMR spectrum matches that were previously reported.³² To this homogeneous solution (1 mL), the amine substrate (1 mmol) was added, and the reaction was heated to 70 °C for the indicated time which was then monitored by ¹H NMR spectroscopy. In cases where the full conversion was observed, 40 mL of water was added to the crude mixture, and the

resulting mixture was then extracted using ethyl acetate (3 × 40 mL). The organic layer obtained was then dried with MgSO₄, filtered, and the product was characterized by NMR spectroscopy.

General procedure for the tandem protocol

The reduction protocol described above was slightly modified by increasing the amount of NaBH₄ to 2 equivalents, and the reaction time to 16 h. After this step, the reaction was allowed to cool to room temperature in a water bath for 30 min, and the internal pressure was slowly released. Mesitylene (internal standard) was added to this mixture and amine, and methanol was quantified. Next, the sample was filtered with a Chromafil syringe filter (with a pore diameter of 0.22 μm). The resulting sample was placed under high vacuum for 4 h in an oil bath at 50 °C to remove the remaining water and methanol. Then, the trifluoroborohydride solution in DMSO (1.2 M, 0.8 mL) was added to the resulting mixture, and the reaction was heated at 100 °C for 12 h. Subsequent NMR characterizations were performed.

Conclusions

Methanol can be efficiently obtained from CO₂ in high yield using amine/formamides as relay molecules. The tandem procedure allows the synthesis of methanol from CO₂ and water, abundant and non-toxic reagents, together with NaBH₄. The reactions proceed in two steps, although it can be completed in tandem, with optimum results obtained using a formamide that is both easily reduced and easily regenerated (Scheme 5). Thus, formanilide, 4-methylformanilide, and 4-methoxyformanilide were found to be ideal substrates for the overall process as they provide intermediate reactivity for the reduction and *N*-formylation reactions. It was found that the NMR chemical shift of the formyl proton (C¹HO) is an excellent indicator of reactivity, which is important in the development of other efficient processes based on this strategy. This strategy could potentially be combined with direct methanol fuel cells (where the CO₂ produced at the anode is known to hamper its overall efficiency) by enabling a recyclable CO₂ pathway and feedback loop to regenerate methanol.

Conflicts of interest

There are no conflicts to declare.

Acknowledgements

We thank the Swiss Competence Center for Energy Research (SCCER) and the Commission for Technology and Innovation (CTI) for financial support. J. U. thanks the Consejo Nacional de Investigaciones Científicas y Tecnológicas (CONICET) for providing a fellowship.

Notes and references

1 A. Álvarez, A. Bansode, A. Urakawa, A. V. Bavykina, T. A. Wezendonk, M. Makkee, J. Gascon and F. Kapteijn, *Chem. Rev.*, 2017, **117**, 9804–9838.

- 2 E. Balaraman, C. Gunanathan, J. Zhang, L. J. W. Shimon and D. Milstein, *Nat. Chem.*, 2011, **3**, 609–614.
- 3 M. Everett and D. F. Wass, *Chem. Commun.*, 2017, **53**, 9502–9504.
- 4 P. G. Jessop, T. Ikariya and R. Noyori, *Chem. Rev.*, 1995, **95**, 259–272.
- 5 A. L. Bonivardi, D. L. Chiavassa, C. A. Querini and M. A. Baltanás, in *Studies in Surface Science and Catalysis*, ed. A. Corma, F. V. Melo, S. Mendioroz and J. L. G. Fierro, Elsevier, 2000, pp. 3747–3752.
- 6 T. Fujitani and I. Nakamura, *Bull. Chem. Soc. Jpn.*, 2002, **75**, 1393–1398.
- 7 A. Erdöhelyi, M. Pásztor and F. Solymosi, *J. Catal.*, 1986, **98**, 166–177.
- 8 M. Sahibzada, D. Chadwick and I. S. Metcalfe, *Catal. Today*, 1996, **29**, 367–372.
- 9 M. Friedrich, S. Penner, M. Heggen and M. Armbrüster, *Angew. Chem.*, 2013, **125**, 4485–4488.
- 10 H. Kusama, K. Okabe, K. Sayama and H. Arakawa, *Appl. Organomet. Chem.*, 2000, **14**, 836–840.
- 11 T. Inoue, T. Iizuka and K. Tanabe, *Appl. Catal.*, 1989, **46**, 1–9.
- 12 S. Kar, A. Goepfert, J. Kothandaraman and G. K. S. Prakash, *ACS Catal.*, 2017, **7**, 6347–6351.
- 13 Z. Han, L. Rong, J. Wu, L. Zhang, Z. Wang and K. Ding, *Angew. Chem., Int. Ed.*, 2012, **51**, 13041–13045.
- 14 A. Kumar, T. Janes, N. A. Espinosa-Jalapa and D. Milstein, *Angew. Chem., Int. Ed.*, 2018, **57**, 12076–12080.
- 15 F. D. Bobbink, F. Menoud and P. J. Dyson, *ACS Sustainable Chem. Eng.*, 2018, **6**, 12119–12123.
- 16 E. Balaraman, Y. Ben-David and D. Milstein, *Angew. Chem., Int. Ed.*, 2011, **50**, 11702–11705.
- 17 E. Balaraman, B. Gnanaprakasam, L. J. W. Shimon and D. Milstein, *J. Am. Chem. Soc.*, 2010, **132**, 16756–16758.
- 18 M.-L. Yuan, J.-H. Xie, S.-F. Zhu and Q.-L. Zhou, *ACS Catal.*, 2016, **6**, 3665–3669.
- 19 M. Stein and B. Breit, *Angew. Chem., Int. Ed.*, 2013, **52**, 2231–2234.
- 20 N. M. Rezayee, D. C. Samblanet and M. S. Sanford, *ACS Catal.*, 2016, **6**, 6377–6383.
- 21 S. Kar, R. Sen, A. Goepfert and G. K. S. Prakash, *J. Am. Chem. Soc.*, 2018, **140**, 1580–1583.
- 22 G. A. Olah, A. Goepfert and G. K. S. Prakash, *J. Org. Chem.*, 2009, **74**, 487–498.
- 23 M. Hulla, G. Laurenczy and P. J. Dyson, *ACS Catal.*, 2018, **8**, 10619–10630.
- 24 F. D. Bobbink, S. Das and P. J. Dyson, *Nat. Protoc.*, 2017, **12**, 417–428.
- 25 C. C. Chong and R. Kinjo, *Angew. Chem., Int. Ed.*, 2015, **54**, 12116–12120.
- 26 T. V. Q. Nguyen, W.-J. Yoo and S. Kobayashi, *Angew. Chem., Int. Ed.*, 2015, **54**, 9209–9212.
- 27 L. Zhang, Z. Han, X. Zhao, Z. Wang and K. Ding, *Angew. Chem.*, 2015, **127**, 6284–6287.
- 28 U. Jayarathne, Y. Zhang, N. Hazari and W. H. Bernskoetter, *Organometallics*, 2017, **36**, 409–416.
- 29 Y. Liu and J. Schwartz, *J. Org. Chem.*, 1993, **58**, 5005–5007.

- 30 S. Narasimhan, S. Madhavan, R. Balakumar and S. Swarnalakshmi, *Synth. Commun.*, 1997, **27**, 391–394.
- 31 S. K. Mandal, S. C. Sau, R. Bhattacharjee, P. Kumar Hota, P. K. Vardhanapu, G. Vijaykumar, R. Govindarajan and A. Datta, *Chem. Sci.*, 2019, **10**, 1879–1884.
- 32 I. Knopf and C. C. Cummins, *Organometallics*, 2015, **34**, 1601–1603.
- 33 L. Hao, H. Zhang, X. Luo, C. Wu, Y. Zhao, X. Liu, X. Gao, Y. Chen and Z. Liu, *J. CO₂ Util.*, 2017, **22**, 208–211.
- 34 U. Wietelmann, M. Felderhoff and P. Rittmeyer, in *Ullmann's Encyclopedia of Industrial Chemistry*, American Cancer Society, 2016, pp. 1–39.
- 35 L. Ouyang, H. Zhong, H.-W. Li and M. Zhu, *Inorganics*, 2018, **6**, 10.
- 36 K. Chen, L. Ouyang, H. Zhong, J. Liu, H. Wang, H. Shao, Y. Zhang and M. Zhu, *Green Chem.*, 2019, **21**, 4380–4387.
- 37 K. Ramya, K. S. Dhathathreyan, J. Sreenivas, S. Kumar and S. Narasimhan, *Int. J. Energy Res.*, 2013, **37**, 1889–1895.
- 38 A. Gopakumar, I. Akçok, L. Lombardo, F. Le Formal, A. Magrez, K. Sivula and P. J. Dyson, *ChemistrySelect*, 2018, **3**, 10271–10276.
- 39 M. Hulla, F. D. Bobbink, S. Das and P. J. Dyson, *ChemCatChem*, 2016, **8**, 3338–3342.
- 40 C. R. Kemnitz and M. J. Loewen, *J. Am. Chem. Soc.*, 2007, **129**, 2521–2528.
- 41 K. B. Wiberg, C. M. Hadad, P. R. Rablen and J. Cioslowski, *J. Am. Chem. Soc.*, 1992, **114**, 8644–8654.
- 42 J. Liebman and A. Greenberg, in *Molecular Structure and Energetics, Structure and Reactivity*, Wiley-VCH, 1989, vol. 7, p. 7.
- 43 T. E. Davies, S. A. Kondrat, E. Nowicka, J. L. Kean, C. M. Harris, J. M. Socci, D. C. Apperley, S. H. Taylor and A. E. Graham, *Appl. Catal., A*, 2015, **493**, 17–24.
- 44 D. Wang, Q. Cai and K. Ding, *Adv. Synth. Catal.*, 2009, **351**, 1722–1726.
- 45 L. Ma'mani, M. Sheykhan, A. Heydari, M. Faraji and Y. Yamini, *Appl. Catal., A*, 2010, **377**, 64–69.